INSTITUTE OF PHYSICS PUBLISHING SEMICONDUCTOR SCIENCE AND TECHNOLOGY

Semicond. Sci. Technol. **22** (2007) 209–213 doi:10.1088/0268-1242/22/3/006

An acoustoelectric single photon detector

V I Talyanskii[1], J A H Stotz[2] and P V Santos[2]

[1] The Cavendish Laboratory, University of Cambridge, Madingley Road, Cambridge CB3 0HE, UK
[2] Paul-Drude-Institut für Festköperelektronik, Hausvogteiplatz 5-7, D-10117 Berlin, Germany

E-mail: vit10@cam.ac.uk

Received 1 November 2006, in final form 11 December 2006
Published 19 January 2007
Online at stacks.iop.org/SST/22/209

Abstract
We propose a novel single photon detector for quantum information processing and for general applications in areas where the detection of ultra weak photon fluxes is required. The detector is also capable of discriminating between different numbers of photons in a light pulse. It uses acoustic charge transport in order to transfer photogenerated electrons and holes to areas where their charge can be detected by single electron transistors. Preliminary experimental results on the fidelity of the acoustic charge transport are presented, which allows us to make estimates of the detector's performance.

1. Introduction

Single photon emission and detection are of paramount importance for the emerging fields of quantum information processing and quantum communication. Developments in these fields have resulted in new requirements for single photon detection. In particular, it is no longer sufficient to simply detect single photons. A detector that can discriminate between different numbers of photons in a light pulse is now required for quantum cryptography [1], optical quantum computation [2, 3] and quantum metrology [4, 5].

In order to meet the demand for discriminating single photon detectors, novel schemes using cryogenic avalanche devices [6–8] and atomic vapours [9, 10] have recently been proposed. While, in general, avalanche photodetectors and photomultipliers are not suitable to discriminate the number of photons in a pulse, the avalanche multiplication in the As impurity band in silicon has been shown to display nearly noise-free multiplication [6]. This avalanche process has been used in a discriminating single photon solid-state photomultiplier (SSPM) [7, 8]. There is, however, a trade-off between the effective quantum efficiency and the dark count rate, which may constitute a noticeable ($\approx$10%) fraction of the total counts if the effective quantum efficiency of the SSPM is close to 90%. Furthermore, SSPM detectors are very sensitive to thermal photons, and very thorough filtering of infrared radiation is required. The atomic vapours proposal [9, 10] is based on the mapping of the number of quanta absorbed in the vapour to the number of atoms in the particular excited state and measuring the latter. The scheme consists of a cell containing a vapour of atoms and a number of auxiliary lasers to both prepare the initial quantum state of the atoms and to control the interaction of the atoms with the radiation fields. This proposal has serious potential problems with the dark count rate as well as the inherent property to operate only at a fixed frequency. The later drawback is hoped to be overcome by transforming the frequency of the incident photons using a nonlinear optical crystal.

A discriminating single photon detection scheme can also be realized using a single electron transistor (SET) for measuring the number of photogenerated electrons or holes [11]. In this case, the single photon sensitivity is provided by the ability of the SET to measure charge at the single electron level. Inherent to such detectors is a trade-off between the photon collection efficiency and the sensitivity of the charge measurement. In order to achieve maximum sensitivity, the photogenerated electron should be placed sufficiently close (within 1 μm) to the input electrode of the SET. This requirement restricts the size of the photon absorption area and leads to poor photon collection efficiencies. If the absorption area is chosen sufficiently large (e.g. 10×10 μm^2) in order to provide high photon collection efficiency, the sensitivity will then be sacrificed to a significant degree. This trade-off hinders achieving the high quantum efficiencies of approximately 99% required for the most demanding applications of single photon detectors in quantum information processing.

Here, we describe a novel method for single photon detection based on the transport of photogenerated electrons and holes by a surface acoustic wave (SAW). In this scheme, the photon absorption area, where the electrons and the holes are generated by an incident light beam, can be made

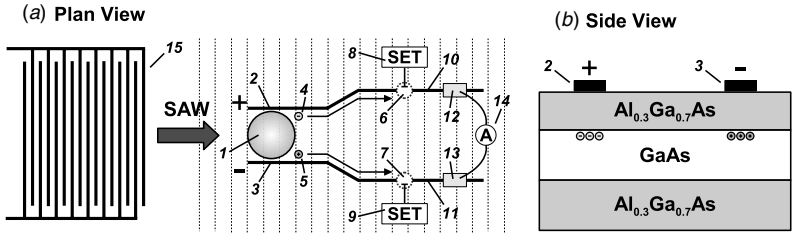

Figure 1. (*a*) Schematic diagram of the photon detector. Incident photons create electron–hole pairs in the absorption region (1). The electrons (4) and holes (5) are spatially separated by an electric field and transported by the SAW along the guides (2) and (3) towards the charge detection areas (6) and (7). (*b*) Semiconductor layer sequence for the detector structure.

sufficiently large in order to provide high photon collection efficiencies. The photogenerated electrons and holes are separately transported by a SAW towards microscopically small charge detection areas, where the charge is measured by a SET. The small size of the charge detection areas ensures that the sensitivity of the measurement of the photogenerated charge is not compromised. Thus, the scheme eliminates the trade off [11] between the sensitivity of the charge detection and the photon collection efficiency.

2. Detector operation

The detector schematic and a possible semiconductor layer sequence for its implementation are shown in figure 1. The GaAs layer, sandwiched between the top and bottom $Al_{0.3}Ga_{0.7}As$ barrier layers (figure 1(*b*)), absorbs the incoming light, for which the top $Al_{0.3}Ga_{0.7}As$ layer is assumed to be transparent. The piezoelectricity of the layers is essential for the operation of the detector.

The primary components of the detector include (figure 1(*a*)): a photon absorption area (1); guides (2, 3) for transporting photogenerated electrons (4) and holes (5) from the absorption area towards the detection areas (6, 7); single electron transistors (8, 9); and an interdigital transducer (IDT, 15) for the generation of a SAW. In this configuration, the photon absorption area can be made sufficiently large (100 μm^2, for example) so that the incident light beam can be easily focused within the area and all incident photons converted into electron–hole pairs. In order to prevent recombination in the absorption layer, the electron–hole pairs are immediately separated by both the piezoelectric field generated by the SAW and an applied dc field in transverse direction. The transverse field provided by the dc voltage applied between the electron and hole guides (2 and 3 in figure 1).

The electrons and holes are attracted to their respective positively and negatively biased guides and then transported by the SAW along the guides towards the microscopically small (<1 μm^2) charge detection areas (6 and 7). In the design shown in figure 1, carrier detection is performed by a SET in the gap between two sections of the electron (hole) guide. The gap represents a potential barrier that electrons (holes) transported by the SAW are unable to cross. The height of the potential barrier can be adjusted by a voltage applied to the second guide sections (10 and 11).

When confined to a small area, a fraction of a square micron, an electron or hole creates a detectable electrostatic potential (on the order of 1 mV), as has been extensively studied in the field of single electronics [12]. The detection areas (6 and 7) are capacitively coupled to SETs 8 and 9, respectively. When the electrons and holes are brought to the detection areas and the charge measurements are completed, the voltage on the second guide sections (10 and 11) is adjusted to become more positive (negative) for the electron (hole) guide to allow the electrons (holes) to be transferred through the gap towards the drain contacts (12 and 13). The charge detection areas are then ready for the next measurement. The number of electrons (holes) detected equals to the number of absorbed photons. An ammeter (14 in figure 1) can optionally be used for weak CW light fluxes.

Charge transport by a SAW therefore allows for a design that combines a large photon absorption area with a microscopic charge detection region that is necessary for charge detection at the single electron level. We discuss a detector based on III–V piezoelectric structures, because the piezoelectricity is essential for the realization of acoustic charge transport (ACT). The energy band gaps of GaAs and (Al,Ga)As determine the detection wavelength range for the structure in figure 1(*b*). The transport of photoinduced electrons and holes is confined to the GaAs layer by the offsets between the conduction and valence bands of GaAs and the (Al,Ga)As barriers. Fortunately, many interesting systems possess piezoelectric properties allowing the implementation of the concept over a wide band of optical wavelengths. In particular, detectors based on the (In,Ga)As/InP material system can operate in the fibre-compatible wavelength of 1550 nm. Moreover, the proposed concept can be extended to nonpiezoelectric materials by using hybrid architectures, where a nonpiezoelectric semiconductor layer is in close proximity to a piezoelectric substrate.

3. Expected characteristics of the detector

There are three basic processes that determine the detector performance: (1) electron–hole pair photogeneration, (2) transportation of the photogenerated charge carriers by the SAW to the charge detection regions and (3) electrical detection of charge at the single electron level.

Photogeneration of electron–hole pairs is common for many light detection schemes, and the main objective is to achieve an efficient absorption of light. High ($>90\%$) levels of absorption are routinely achieved in optical devices. The spatial separation of the absorption and detection areas inherent to our scheme facilitates optimization of the photon absorption process.

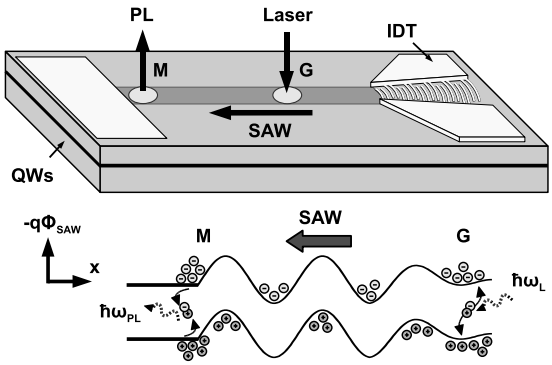

Figure 2. Schematic representation of the transport of electrons and holes by the SAW potential in GaAs QWs. The SAW generated by an IDT deposited on the sample surface creates a piezoelectric potential Φ_{saw}, which spatially separates electrons and holes generated by a laser spot in position G. The carriers are transported by the moving SAW potential to the edge of a metal stripe M. The metal short circuits the piezoelectric field, thus allowing the carriers to recombine. The resulting luminescence at M is used to measure the transport efficiency.

Process (3), single electron detection, determines the operating speed of the detector. At present, the best choice for the SET is a radio frequency single electron transistor (RF-SET) [13], which is the fastest electrometer currently available. The speed and sensitivity of the charge measurement can be improved by using low-noise, cryogenic RF amplifiers (that follow the RF-SETs as a second stage amplifiers) and by optimizing the coupling between the SET and the RF resonant circuit in which the SET is embedded. In this way, the sensitivity becomes limited only by the shot noise of the SET. Under these conditions, it should be possible to reach read-out times around 100–200 ns, corresponding to a bandwidth approaching 10^7 Hz.

Process (2), the acoustic transport of carriers to the charge detection region, has not been used before in the context of light detection and could potentially limit the quantum efficiency and the sensitivity of the detector. A trap present near guide 2 (figure 1) can capture an electron (or a hole for guide 3) transported along the guide by a SAW. The trap could hold the electron for an unspecified time and then release it into a later SAW potential minimum. A sufficiently long trap holding time (as compared with the time interval between subsequent light pulses) would be perceived in the detector response to be a dark count event.

The fidelity of the ACT can be characterized by the distance (L_{charge}) over which a SAW potential well travels while conserving its charge; L_{charge} depends on the quality of the semiconductor structure and on the SAW amplitude. The requirements on L_{charge} vary, of course, with the particular application. In order to assess the effect of the ACT on the detector characteristics, we have performed preliminary measurements of L_{charge}. Our experiment uses a spatially resolved photoluminescence (PL) technique to assess the ACT, as illustrated in figure 2. The electrons and holes photogenerated at position G are spatially separated and transported by the SAW towards a metal stripe that short-circuits the piezoelectric field, thus allowing the electrons and holes to approach each other and recombine. The intensity of the PL at the metal stripe depends on the charge loss during the transportation. By changing the distance between the generation (G) and the detection point (M, at the edge of the metal stripe), L_{charge} can be measured. This setup also allows the study of PL along the transport path in order to locate trapping sites that may compromise the ACT. The results, however, indicate that a high acoustoelectric charge transport is indeed achievable.

The PL experiments were performed on a sample containing three $Al_{0.3}Ga_{0.7}As/GaAs$ quantum wells (QWs) with thicknesses of 12, 15 and 20 nm and located between 150 and 200 nm below the surface of the sample. Such a structure allows the investigation of the dependence of L_{charge} on the QW width. A focusing split-finger IDT deposited on top of the layer stack generates a SAW propagating along the [1 1 0] direction of the (1 0 0) surface. The IDTs have been designed for operation at an acoustic wavelength $\lambda_{\mathrm{SAW}} = 5.6\ \mu$m, corresponding to a frequency of 520 MHz. The continuous radiation from a frequency doubled Nd:YAG laser ($\lambda = 532$ nm) focused onto a 2 μm spot at position G was used for optical excitation. The PL emitted along the transport path was directed to a grating spectrometer and detected using an intensified charge coupled device camera.

Figure 3 shows spatial profiles of the PL intensity I_{PL} for the three QWs, obtained with the exciting laser beam approximately 30 μm away from the metal. I_{PL} was integrated across a narrow strip (approximately 1 μm wide) along the centre of the SAW beam and normalized to the PL intensity at G in the absence of a SAW, $I_{\mathrm{PL},0}$. Under a SAW, the PL intensity at the excitation point G is considerably reduced in comparison with the value obtained in the absence of the SAW (to approximately 18% of the initial intensity for QW1). This reduction is attributed to the spatial separation of the carriers and their transport away from G. During ACT, the widest QW (QW1) only shows PL at G and near the metal edge M resulting from induced electron–hole recombination. The absence of PL between G and M indicates that transport within this QW is insensitive to defects. The narrowest QW (QW3) shows, in contrast, two prominent features denoted as D1 and D2, at distances of 7 and 15 μm from the metal, respectively. These structures are attributed to radiative defects along the transport path, which initially capture carriers of one polarity. Radiative recombination from these defects occurs when the SAW field brings carriers of opposite polarity to the defect. Furthermore, we note that the ratio between the PL intensities at M and G is much smaller for QW3 than for QW1 due to recombination losses during transport.

In order to determine the charge transport length, we measured the PL intensity near the metal stripe M for different distances d_{G} between M and the generation point G (inset of figure 3). The variations in the PL intensity near the metal directly reflect the carrier losses along the transport path. Interestingly, for all QWs, the PL intensity does not decrease monotonically with d_{G}, but remains relatively constant for $d_{\mathrm{G}} > 15\ \mu$m, thus implying a long L_{charge}. The PL measured at the generation point does, however, decrease when the carriers are photogenerated in the vicinity of defects D1 and D2. These results show that photogenerated electrons and holes can be acoustically transported over long distances with negligible losses due to recombination. In fact, carrier transport over

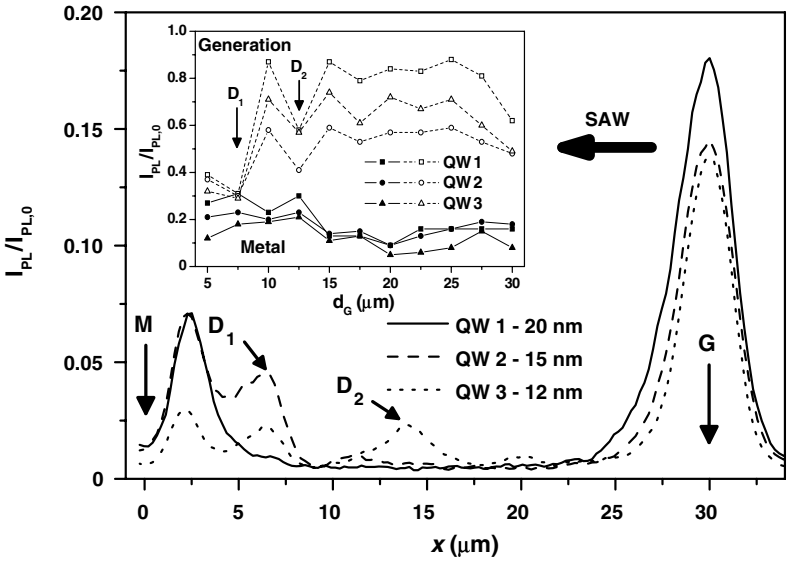

Figure 3. Photoluminescence emitted by QW1 (solid line), QW2 (dashed line) and QW3 (dotted line) along the SAW propagation path. The electron and holes are generated by a laser spot at position G and transported by the SAW to the detection spot M at the edge of a metal stripe. D1 and D2 denote radiative defects on the SAW path. For each QW, the PL is normalized to the maximum value in the absence of a SAW. Inset: PL intensity at the generation point G (open symbols) and close to the metal edge M (solid symbols) as a function of the distance d_G between G and M.

several hundreds of microns has been observed [14]. The PL measurements also indicate that narrower QWs are more susceptible to defects than wider ones. Although further studies are necessary to clarify the mechanism responsible for that dependence, it seems that the density of defects and their effect on transport can be reduced by an appropriate design of the layer structure.

Taking into consideration the three processes that govern the efficiency of our proposed detector, we can make a rough estimate of the upper bound for the quantum efficiency and the rate of 'wrong counts' imposed by the acoustic transport on a detector with the same fidelity as in the experiment in figures 2 and 3. The sensitivity of the optical detectors used in our experiment was approximately 10^4 photons per second. No photons emitted from traps were observed for ACT in QW1 suggesting that the number of photons (if any) emitted from the traps in the ACT path was less than 10^4 photons per second.

If we assume that each trapped electron or a hole causes a photon emission, then as a rough estimate, we obtain the rate of the trapping events in our PL experiments (figure 2) to be around 10^4 per sec. This estimate neglects the non-radiative recombination of the trapped electrons and holes and the events in which an electron (a hole) is trapped and then released by the trap.

In the acoustoelectric detector the trapping events do not lead to the recombination because the electron and hole paths are separated. Nevertheless such events deteriorate the detector performance. A trapped electron arrives to its charge detection region with some delay and causes the SET to make a count at a 'wrong' time. If the delay is comparable or larger than the time between consecutive light pulses, then the 'wrong time' readings do not provide any useful information and in fact obscure the 'correct' readings caused by electrons that reached the SET without delay. The same considerations apply to the holes that are transported along their own ACT path and measured by a separate SET (figure 1). Thus the 'wrong time' SET readings act and will be perceived as dark count events despite that they are caused in the first place by the photons that have to be detected.

In order to estimate the detector's 'wrong time' readings rate we assume that the rate of the trapping events in the detector is similar to that in the QW structures used in our PL experiments (figure 2). Such assumption leads to around 10^4 'wrong time' readings of the detector per second. The acoustoelectric detector is expected to be able to count photons at the rate of 10^6 light pulses per second. In this regime, the rate of the 'wrong time' readings (normalized to the repetition rate of a true signal) will be below 0.01. This performance would satisfy the requirements of linear optics quantum computing according to the scheme suggested in [2], where the photon counting device must produce less than one false count per each 100 true counts.

The detector readings caused by the photogenerated carriers that have been trapped during the process of charge transport should be discarded. It is equivalent to 1% of the photons being lost and would result in the corresponding small (1%) decrease of the quantum efficiency. In practical terms, the quantum efficiency of the detector will therefore be determined by the efficiency of the photon collection process rather than by the ACT.

4. Conclusions

We propose a design of a single photon detector capable of counting the number of photons in a light pulse. Using acoustic charge transport, this design allows electrons and holes photogenerated in a large absorption area to be brought to smaller regions of the device suitable for detection by single electron transistors. Preliminary experiments on the fidelity of the acoustic charge transport indicate that the characteristics

of the detector will make it suitable for quantum information processing applications.

Acknowledgments

VT thanks G Milburn for discussions concerning applications of discriminating photon detectors. We also thank R Hey and M Höricke for the growth of the quantum well structures. This work has been supported by the EC ACDET II program. VT acknowledges support from the Newton Trust.

References

[1] Gisin N, Ribordy G, Tittel W and Zbinden H 2001 *Preprint* quant-ph/0101098
[2] Knill E, Laflamme R and Milburn G J 2001 *Nature* **409** 46
[3] Online at http://qist.lanl.gov
[4] Sanders B C and Milburn G J 1995 *Phys. Rev. Lett.* **75** 2944
[5] Shapiro J H 1993 *Phys. Scr. T* **48** 105
[6] Kim J, Takeuchi S, Yamamoto Y and Hogue H H 1999 *Appl. Phys. Lett.* **74** 902
[7] Petroff M D, Stapelbroek M G and Kleinhans W A 1997 *Appl. Phys. Lett.* **51** 406
[8] Takeuchi S, Kim J, Yamamoto Y and Hogue H H 1999 *Appl. Phys. Lett.* **74** 1063
[9] Imamoglu A 2002 *Phys. Rev. Lett.* **89** 163602
[10] James D V F and Kwiat P G 2002 *Phys. Rev. Lett.* **89** 183601
[11] Cleland A N, Esteve D, Urbina C and Devoret M H 1992 *Appl. Phys. Lett.* **61** 2820
[12] Grabert H and Devoret M 1992 *Single Charge Tunneling, Coulomb Blockade Phenomena in Nanostructures* (New York: Plenum)
[13] Schoelkopf R J, Wahlgren P, Kozhevnikov A A, Delsing P and Prober D E 1998 *Science* **280** 1238
[14] Alsina F, Stotz J A H, Hey R and Santos P V 2004 *Solid State Commun.* **129** 453